Composite Nature of Layered Hybrid Perovskites : Assessment on Quantum and Dielectric Confinements and Band Alignment

(Supplementary Information)

Boubacar Traore,[*,†] Laurent Pedesseau,[‡] Linda Assam,[‡,¶] Xiaoyang Che,[†,‡] Jean-Christophe Blancon,[§] Hsinhan Tsai,[§] Wanyi Nie,[§] Constantinos C. Stoumpos,[∥] Mercouri G. Kanatzidis,[∥] Sergei Tretiak,[§] Aditya D. Mohite,[§] Jacky Even,[‡] Mikaël Kepenekian,[*,†] and Claudine Katan[*,†]

†*Univ Rennes, ENSCR, INSA Rennes, CNRS, ISCR (Institut des Sciences Chimiques de Rennes) - UMR 6226, F-35000 Rennes, France*

‡*Univ Rennes, INSA Rennes, CNRS, Institut FOTON - UMR 6082, F-35000 Rennes, France*

¶*TOTAL SA, Tour Coupole, 2 place Jean Miller - La Défense 6 - Courbevoie, France*

§*Los Alamos National Laboratory, Los Alamos, NM 87545, USA*

∥*Department of Chemistry, Northwestern University, Evanston, IL 60208, USA*

E-mail: boubacar.traore@univ-rennes1.fr; mikael.kepenekian@univ-rennes1.fr; claudine.katan@univ-rennes1.fr

S1 Band structure with and without Cs replacement

In the composite approach as discussed in the main manuscript, the 2D HOP is regarded as a composite material whereby one can define three model structures as shown in the manuscript. To model the perovskite structure (W) from the composite ($BA_2(MA)_4Pb_5I_{16}$), the inter-layer molecules butyl-ammonium (BA) were replaced by Cs ($Cs_2(MA)_4Pb_5I_{16}$). These molecular states do not contribute or less in the band egde. Indeed, as some of us have previously demonstrated,[1–3] the organic molecules have states either too high in the conduction band (CB) or too deep in the valence band (VB). As such, they may be replaced by an inorganic cation such as Cs^+ so as to mimic the Coulomb interactions with the inorganic layer without altering much the band structure close to the electronic gap. This is verified in the band structure of n=5 with and without Cs replacement as shown in Figure **S1**.

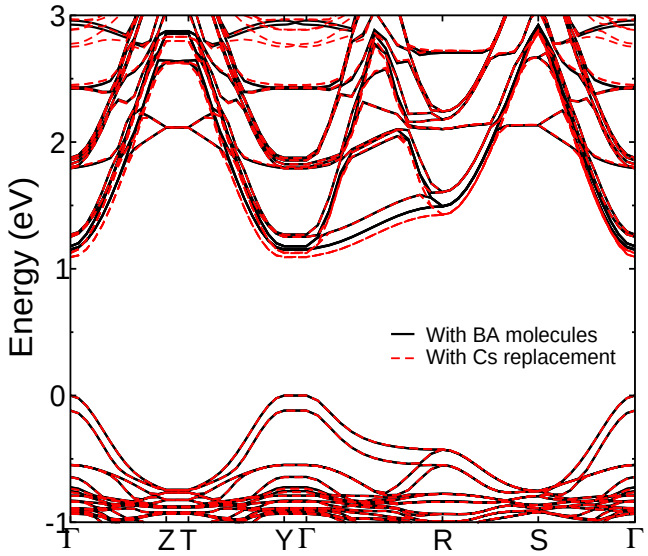

Figure S1: Comparison of the band structures of n=5 $(BA)_2(MA)_4Pb_5I_{16}$ member of 2D HOP RP phases[4] with and without Cs replacement. Spin-orbit coupling is not included in the calculations.

S2 Composite nature of dielectric profiles in 2D HOP

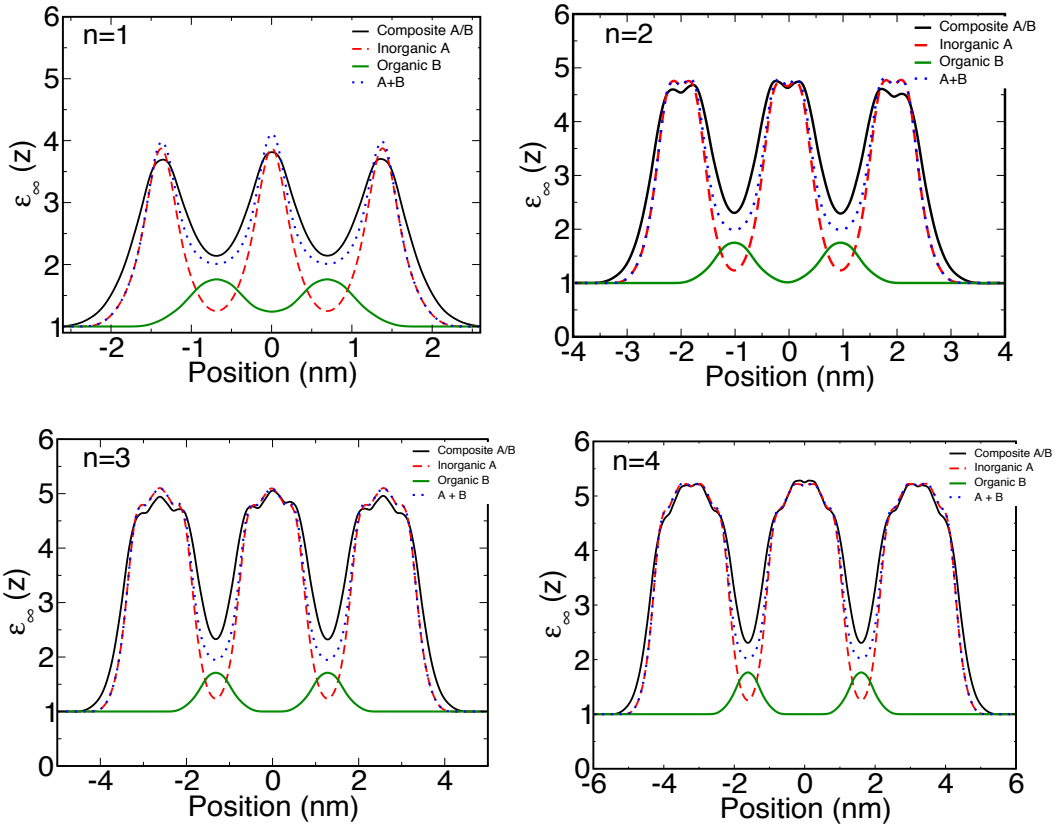

Figure S2: Composite nature of high-frequency dielectric constant applied to n=1-4 member of 2D RP HOP. We notice a larger mismacth of the profiles at the inorganic layer when n=1.

S3 Definition of octahedral tilt angles (β, δ)

The octahedral tilt angles are defined as shown in Figure **S3**.[5] These angles allow to rationalize the interplay between structural distortions and optoelectonic properties of hybrid organic-inorganic perovskites.

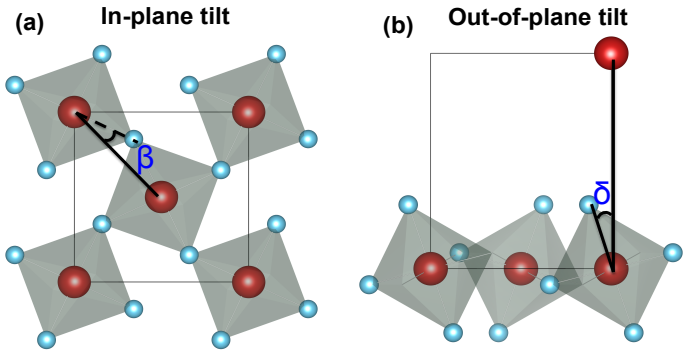

Figure S3: Definition of the octahedral tilt angles.[5] a) In-plane tilt angle β and (b) out-of-plane tilt angle δ.

S4 Chemical tuning of the inorganic well

Table S1: Octahedral distorsion angles (β, δ) and space groups of $(PMA)_2PbX_4$ series of 2D perovskites.

	β (^{o})	δ (^{o})	space group
$(PMA)_2PbI_4$	10.1	8.3	Pbca
$(PMA)_2PbBr_4$	15.0	4.3	Pbca
$(PMA)_2PbCl_4$	15.9	6.0	Cmc21

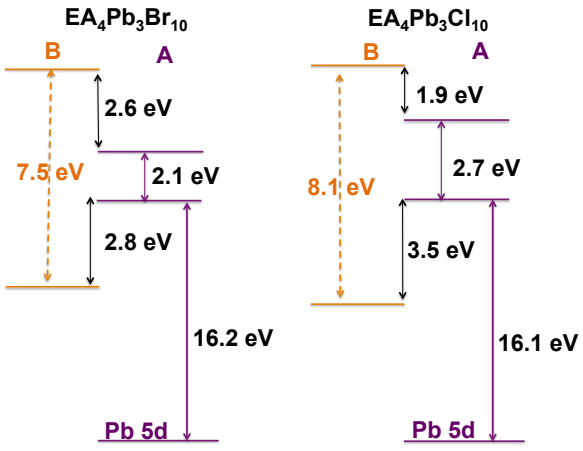

Figure S4: a) Band alignment of $(EA)_4Pb_3X_{10}$ series of 2D HOP showing the different band offsets. X refers to the halogens Br and Cl. DFT band gaps are used to align the CB.

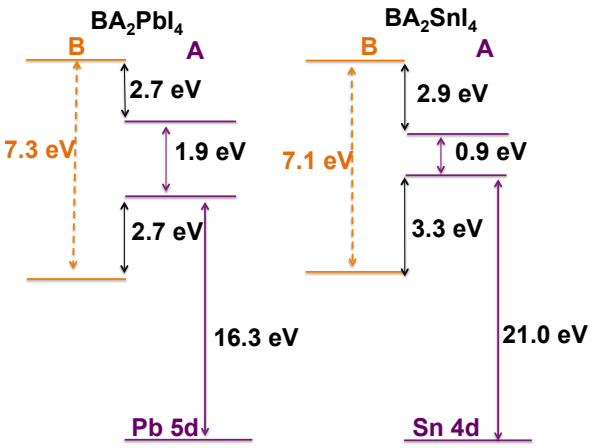

Figure S5: Band alignment of $(BA)_2MI_4$ series of 2D HOP showing the different band offsets. M refers to the metals Pb and Sn. DFT band gaps are used to align CBM.

S5 Effect of the barrier length

Table S2: Octahedral distorsion angles (β, δ) and in-plane lattice parameters of $(C_mH_{2m+1}NH_3)_2PbI_4$ series of 2D perovskites. Cm refers to a system with m carbon atoms in the alkyl chain.

	a (Å)	b (Å)	β (^{o})	δ (^{o})	Space group
C4	8.8764	8.6925	12.3	5.8	Pbca
C6	8.9413	8.6874	12.0	5.8	Pbca
C8	8.9817	8.6886	11.7	6.1	Pbca
C10	8.9708	8.6733	12.0	6.1	Pbca
C12	8.8645	8.5149	11.5	11.2	Pbca
C16	8.8167	8.5222	11.9	11.1	Pbca
C18	8.7825	8.5401	12.0	11.0	Pbca

S6 Effect of lattice distortion related to structural phase transitions

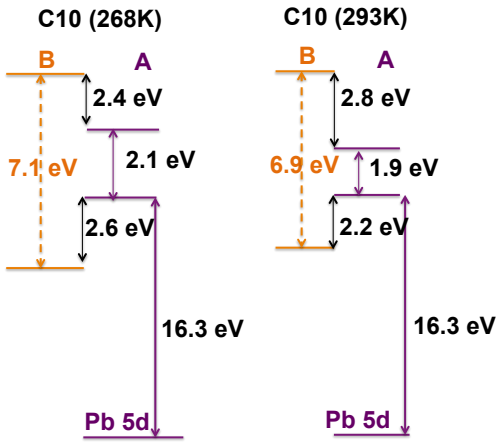

Figure S6: Band alignment of C10 [$(C_{10}H_{21}NH_3)_2PbI_4$] showing the effect of phase transition on the confinement potentials. DFT band gaps are used.

Table S3: Octahedral distorsion angles (β, δ) and in-plane lattice parameters of C10 [$(C_{10}H_{21}NH_3)_2PbI_4$] showing the effect of phase transition.

	a (Å)	b (Å)	β (^{o})	δ (^{o})
C10 (268 K)	8.8314	8.4871	11.9	11.1
C10 (293 K)	8.9708	8.6733	12.0	6.1

S7 Effect of well's thickness

Table S4: Data summarizing the space group, inorganic layer thickness of the n=1-5 members of 2D RP HOP ($(BA)_2(MA)_{n-1}Pb_nI_{3n+1}$) and exciton reduced masses used to calibrate the $0.200m_0$ adopted for the effective mass approximation.

n	Space group	well thickness (Å)	exp. exciton reduced mass in m_0 unit[6]
1	Pbca	6.41	0.184
2	Cmcm	12.55	0.217
3	Cmca	18.92	0.201
4	Cmcm	25.11	0.196
5	Aba2	31.39	0.20

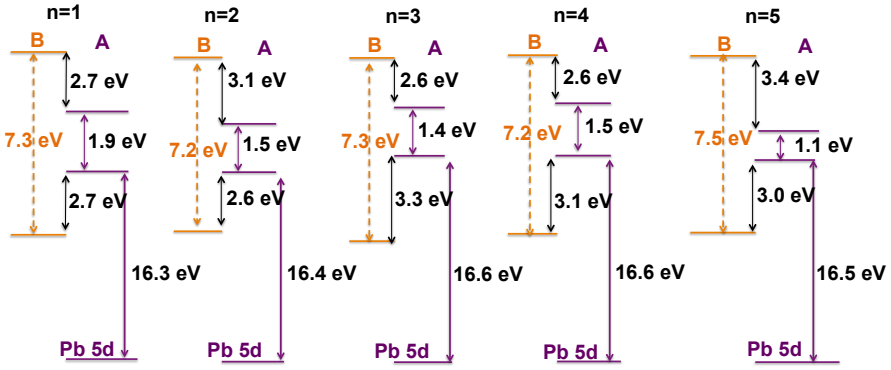

Figure S7: Band alignment of n=1 to 5 members of 2D RP HOP ($(BA)_2(MA)_{n-1}Pb_nI_{3n+1}$) showing the different band offsets. DFT band gaps are used.

S8 Note on band alignment with monolayered (n=1) structures

As mentioned in the main manuscript, the difference between the Hartree potentials (ΔV_H) and Pb 5d (ΔE_{5d}) states amounts to 0.14 eV for 2D RP n=1. For other monolayered structures (n=1) , this difference varies between 0.1 eV and 0.15 eV. As such, the error in

hole confinement potentials also falls in the same range. We noticed, however, that the shift between the Pb 5d states from W/B and B is about the same shift as between $\mathrm{VBM}_{W/B}$ and VBM_{W}. Given that Pb 5d states are low-lying orbitals unaffected by chemical substitution that can be used as electronic markers,[1] we applied the ΔE_{5d} shift value to VBM for VB alignment (keeping in mind the 0.1 eV to 0.15 eV error).

S9 Parameters used in the effective mass approximation

Table S5: Effective masses used to fit the experimental continuum band gaps of n=1-5 members of 2D HOP ($(\mathrm{BA})_2(\mathrm{MA})_{n-1}\mathrm{Pb}_n\mathrm{I}_{3n+1}$) within the effective mass approximation.

	Well		Barrier	
n	m_e	m_h	m_e	m_h
1	0.105	0.220	0.650	0.650
2	0.105	0.220	0.650	0.650
3	0.100	0.150	0.500	0.500
4	0.080	0.100	0.300	0.300
5	0.080	0.100	0.200	0.300

S10 Used experimental band gaps

Table S6: Experimental band gaps used for the conduction band (CB) alignment.

section	Structures	Band gap (eV)	Reference
Tuning of the inorganic well	$(PMA)_2PbCl_4$	3.65	7
	$(EA)_4Pb_3Br_{10}$	2.75	8
	$(EA)_4Pb_3Cl_{10}$	3.45	8
	$(BA)_2PbI_4$	2.80	9
	$(BA)_2SnI_4$	1.83	10
Effect of the perovskite layer thickness $(BA)_2(MA)_{n-1}Pb_nI_{3n+1}$	n=1	2.80	9
	n=2	2.44	9
	n=3	2.26	9
	n=4	2.15	9
	n=5	2.08	9

References

1. Even, J.; Pedesseau, L.; Jancu, J.-M.; Katan, C. Importance of Spin-Orbit Coupling in Hybrid Organic/Inorganic Perovskites for Photovoltaic Applications. *J. Phys. Chem. Lett.* **2013**, *4*, 2999–3005.

2. Pedesseau, L.; Jancu, J.-M.; Rolland, A.; Deleporte, E.; Katan, C.; Even, J. Electronic Properties of 2D and 3D Hybrid OrganicInorganic Perovskites for Optoelectronic and Photovoltaic Applications. *Optical and Quantum Electronics* **2014**, *46*, 1225–1232.

3. Katan, C.; Pedesseau, L.; Kepenekian, M.; Rolland, A.; Even, J. Interplay of Spin-Orbit Coupling and Lattice Distortion in Metal Substituted 3D Tri-Chloride Hybrid Perovskites. *J. Mater. Chem. A* **2015**, *3*, 9232–9240.

4. Stoumpos, C. C.; Soe, C. M. M.; Tsai, H.; Nie, W.; Blancon, J.-C.; Cao, D. H.;

Liu, F.; Traoré, B.; Katan, C.; Even, J. *et al.* High Members of the 2D Ruddlesden-Popper Halide Perovskites: Synthesis, Optical Properties, and Solar Cells of $(CH_3(CH_2)_3NH_3)_2(CH_3NH_3)_4Pb_5I_{16}$. *Chem* **2017**, *2*, 427 – 440.

5. Pedesseau, L.; Sapori, D.; Traore, B.; Robles, R.; Fang, H.-H.; Loi, M. A.; Tsai, H.; Nie, W.; Blancon, J.-C.; Neukirch, A. *et al.* Advances and Promises of Layered Halide Hybrid Perovskite Semiconductors. *ACS Nano* **2016**, *10*, 9776–9786.

6. Blancon, J.-C.; Stier, A. V.; Tsai, H.; Nie, W.; Stoumpos, C. C.; Traoré, B.; Pedesseau, L.; Kepenekian, M.; Tretiak, S.; Crooker, S. A. *et al.* Unusual Thickness Dependence of Exciton Characteristics in 2D Perovskite Quantum Wells. *ArXiv e-prints* **2017**,

7. Liao, W.-Q.; Zhang, Y.; Hu, C.-L.; Mao, J.-G.; Ye, H.-Y.; Li, P.-F.; Huang, S. D.; Xiong, R.-G. A Lead-Halide Perovskite Molecular Ferroelectric Semiconductor. *Nat. Commun.* **2015**, *6*, 1–7.

8. Mao, L.; Wu, Y.; Stoumpos, C. C.; Traore, B.; Katan, C.; Even, J.; Wasielewski, M. R.; Kanatzidis, M. G. Tunable White-Light Emission in Single-Cation-Templated Three-Layered 2D Perovskites $(CH_3CH_2NH_3)_4Pb_3Br_{10x}Cl_x$. *J. Am. Chem. Soc.* **2017**, *139*, 11956–11963.

9. Blancon, J.-C.; Tsai, H.; Nie, W.; Stoumpos, C. C.; Pedesseau, L.; Katan, C.; Kepenekian, M.; Soe, C. M. M.; Appavoo, K.; Sfeir, M. Y. *et al.* Extremely Efficient Internal Exciton Dissociation Through Edge States in Layered 2D Perovskites. *Science* **2017**, *335*, 1288–1292.

10. Cao, D. H.; Stoumpos, C. C.; Yokoyama, T.; Logsdon, J. L.; Song, T.-B.; Farha, O. K.; Wasielewski, M. R.; Hupp, J. T.; Kanatzidis, M. G. Thin Films and Solar Cells Based on Semiconducting Two-Dimensional Ruddlesden-Popper

$(CH_3(CH_2)_3NH_3)_2(CH_3NH_3)_{n-1}Sn_nI_{3n+1}$ Perovskites. *ACS Energy Lett.* **2017**, *2*, 982–990.